NUMERICAL VALIDATION OF THE COMBINED EXTRUSION-SPLITTING PROCESS OF ENERGY ABSORPTION THROUGH EXPERIMENTAL STUDY

J. Tanasković[a,*], F. Franklin[b], A. Dišić[c], Ž. Mišković[a],

[a] University of Belgrade, Faculty of Mechanical Engineering, Kraljice Marije 16, Belgrade, Serbia

[b] Newcastle University, Newcastle upon Tyne, NE1 7RU, UK

[c] University of Kragujevac, Faculty of Engineering, Sestre Janjić 6, Kragujevac, Serbia

Corresponding author: J. Tanasković, Kraljice Marije 16 Street, 11000 Belgrade, Serbia, Phone: +381 64 12 32 854, Fax: +381 11 3370 364, E-mail: jtanaskovic@mas.bg.ac.rs

Abstract

This paper describes validation process of numerical model of combined collision kinetic energy absorber of rail vehicles based on results of experimental investigations. Combined absorber works on the principle of extrusion-splitting the seamless tube. With the aim to choose the most appropriate tube geometry, the tubes of the different geometry of cross section were made and tested. Key geometry parts have the shape and length of the grooves along the inner tube wall. During the second phase of deformation comes to controlled splitting of the tube wall along these grooves. Experimental and numerical investigations were realized on the scaled samples. Using this type of absorber energy absorption occurs by friction between absorption elements and elastic-plastic deformation of the tube. Combining of two deformation processes gives a higher absorption power as well as compact dimensions of absorber which can be installed in a very limited space in the front part of the vehicle structure. Creating of the numerical model and numerical simulations of extrusion-splitting processes were realized using SolidWorks and ANSYS LS Dyna software packages. Results of experimental investigations and numerical simulations show very good agreement which verifies developed numerical model for use in further investigations in this field.

Keywords: Numerical Simulations, Experimental Study, Extrusion, Splitting, Rail Vehicles

Acknowledgement: The research work is funded by the Ministry of Education, Science and Technological Development of Republic of Serbia, Projects TR35045 and TR35006.

1. Introduction

Wagons are complex structures with very little space for mounting passive safety elements. The size of an impact energy absorber generally increases with the required absorption power [1], but depends also on the geometry of the absorber and the mounting arrangement. The purpose of the absorber is to protect the wagon, and it must be mounted in a way that prevents distortion of the wagon's structure [2]. In the event of a collision, the absorber undergoes controlled deformation, converting the kinetic energy to heat through friction and plastic deformation and reducing the impact force transmitted to the wagon.

One design of absorber that has been studied in the past is based on plastic extrusion of a seamless tube [3–6]. The impact forces the tube into a conical bushing and through an aperture with a smaller diameter. The force vs. stroke characteristics are very good, increasing smoothly to a maximum at the point when the tube is being fully compressed, and remaining at the maximum with only minor deviation while the length of the tube is pushed through. The principal disadvantage of this design is that an increase in absorption power requires an increase in length of the tube – which is generally not possible with the limited space available on the wagon structure.

Another way to increase the absorption power is to combine the extrusion process with a second process that does not require additional space, and that produces controlled deformation and does not induces sharp peaks in the transmitted force. Folding and splitting are two possibilities.

Splitting of the tube, and the influence of tube diameter and the number of grooves, has been studied theoretically and experimentally in quasi-static tests using aluminium and steel tubes with different thicknesses and lengths [7–9]. The grooves along the inner wall of the tube create paths for controlled longitudinal cracking during deformation. After a sharp peak at the start of the splitting process, the force decreases to the half of the start value and remains at that value with minor deviations to the end of the splitting process. The force increases with number of the grooves, and it is possible to influence the shape of deformation (splitting) using different angles of the splitting tool. A larger angle of the cone on the splitting tool increases the deformation resistance. The smoothness of the transmitted force and the absorption power depend on tube wall thickness and quality of material.

Analyses of different types of deformation, such as bending, axial loading, buckling and splitting of the tubes were presented in Ref. [10]. Results of these investigations reveal peaks of the force at the start of deformation process; the design objective of an absorber is to prevent the high peak forces that can produce plastic (permanent) deformation of the vehicle structure behind the absorption elements. Pre-deformation of the tube can reduce the peak

at the start of deformation process, as can the grooves along the length of the inner tube wall that guide propagation of cracks and the formation of the strips.

The influence of impact speed on the deformation resistance of absorption elements that work on the principle of folding the tube, as well as finite element analysis of the deformation, were presented in Ref. [11]. This type of deformation is a form of buckling and gives a characteristic jagged effect to the force vs. stroke measurement. Another way to increase absorption power is to use a foam-filled tube [12]. This reduces the jagged effect, but does not eliminate the peak force at the start. A combined absorber that uses the extrusion-folding process of deformation can be compact and can give higher absorption power but cannot eliminate the peak at the start of deformation of each segment of the tube [13].

Bearing in mind the advantages and disadvantages of each type of deformation, the combination of extrusion-splitting of a seamless tube, with a grooved cylindrical section, is a good potential solution. The splitting process, as a method of deformation in the second phase of energy absorption, demands less mounting space in comparison with the folding process, and the grooves reduce the peak in transmitted force at the start of deformation.

Fig. 1 shows the working principle of the combined absorber. During collision, energy absorption starts with extrusion of the tube (Item 1) by compressing it through the cone bushing (Item 2). After a precisely defined stroke, the process of splitting the part of the tube that has passed through the cone bushing starts using a special splitting tool (Item 3). From that moment, the extrusion and splitting processes work in parallel until the tube material has been fully used. Energy absorption occurs by elastic-plastic deformation of the tube, and friction between the tube and first the cone bushing and later the splitting tool.

Numerical simulations have been performed using ANSYS LS-Dyna and verified using experimental results. The numerical model developed here can be used for further dimensioning of this type of absorber without the need for additional experimental investigations, thereby greatly reducing development-design costs. This type of absorber can be installed in a line with the standard buffer on passenger, freight and locomotives, or can be used as a separate assembly installed in a front part of a railway vehicle structure.

The experimental investigations presented in this paper used scaled samples. Results of the experimental investigations and numerical simulations are in a good agreement, with acceptable deviations, in the first and second phases of energy absorption.

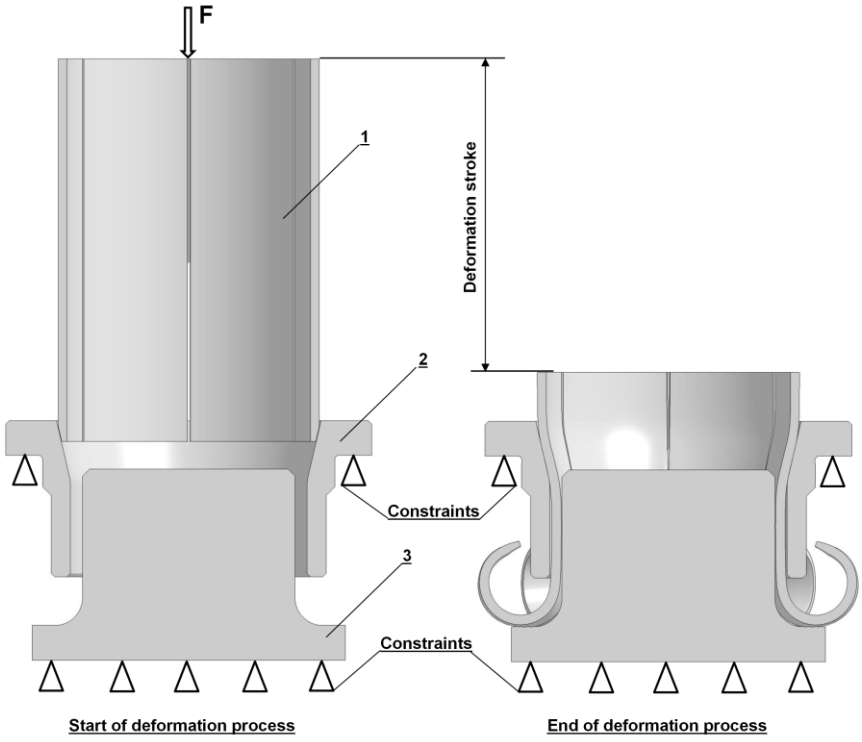

Figure 1 Working principle of combined absorber: (1- Seamless grooved tube, 2- Cone bushing and 3-Splitting tool)

2. Experimental study

Quasi-static tests were performed in laboratory conditions at the Faculty of Mechanical Engineering University of Belgrade, using a servo-hydraulic machine ZWICK ROELL HB250 (see Fig. 2) that can apply a maximum load of 250 kN. Tests were performed with a piston speed of 1 mm/s. During the tests, the stroke was pre-set and deformation resistance measured during the defined stroke. The research presented in this paper is based on previous investigations of collision energy absorbers [3–6, 13]. Experimental and numerical results obtained in these investigations have shown that absorption power and shape of deformation can be studied in a quasi-static environment and used as a base for further dimensioning of absorption elements in full-scale testing, e.g., through collision of two passenger wagons.

Figure 2 Servo-hydraulic machine ZWICK ROELL HB250

2.1. Working principles

During collision, the energy absorption begins with compression of the tube (Item 1 in Fig. 1) through the cone bushing (Item 2). This first phase has a stroke of 50 mm, ending when the splitting tool (Item 3) comes into contact with the narrowed part of the tube. From that point on, extrusion and splitting work in parallel, for a further 40mm of stroke (i.e., total stroke length is 90 mm).

2.2. Samples

Samples made for the experimental investigations are shown in Fig. 3: seamless tubes with dimensions ∅75/70, length L = 110 mm (Items 1, 2 and 3) from low carbon steel (material P235T1); cone bushing (Item 4 and 5) with dimensions ∅75/68x13°; and splitting tool (Item 6) with dimensions ∅61/r8 from quenched and tempered carbon steel (material C45E). The seamless tubes are separated in three groups according to geometry of grooves: (a) seamless tubes with grooves on the inner wall of length 110 mm (Item 3); (b) seamless tubes (Item 2) with grooves on the inner wall of length 10 mm and c) seamless tubes (Item 1) without grooves on the inner wall which were used for the control tests and for extrusion-only process as a basis for evaluation of the combined process.

Cone bushings are separated in two groups: a) smaller cone angle bushing (Item 4) which was used for controlled tests and for extrusion-only process and b) larger cone angle bushing (Item 5) which was used for combined process of energy absorption.

Considering the design given in Ref. [8], the number of grooves on the inner tube wall was chosen as an optimal solution so six grooves were made on the inner wall of all tube samples.

Figure 3 Samples: (1-Seamless tube without grooves, 2-Seamless tube with grooves length of 10 mm, 3-Seamless tube with grooves length of 110 mm, 4-Smaller cone angle bushing, 5-Larger cone angle bushing and 6-Splitting tool)

Fig. 4 shows the main dimensions of the samples. All seamless tubes have the same basic dimensions; only the grooves differ between samples. Samples remarked in Fig. 3 (Items 1 to 3) have the same dimensions but grooves length is different for Items 2 and 3, and Item 1 has no grooves.

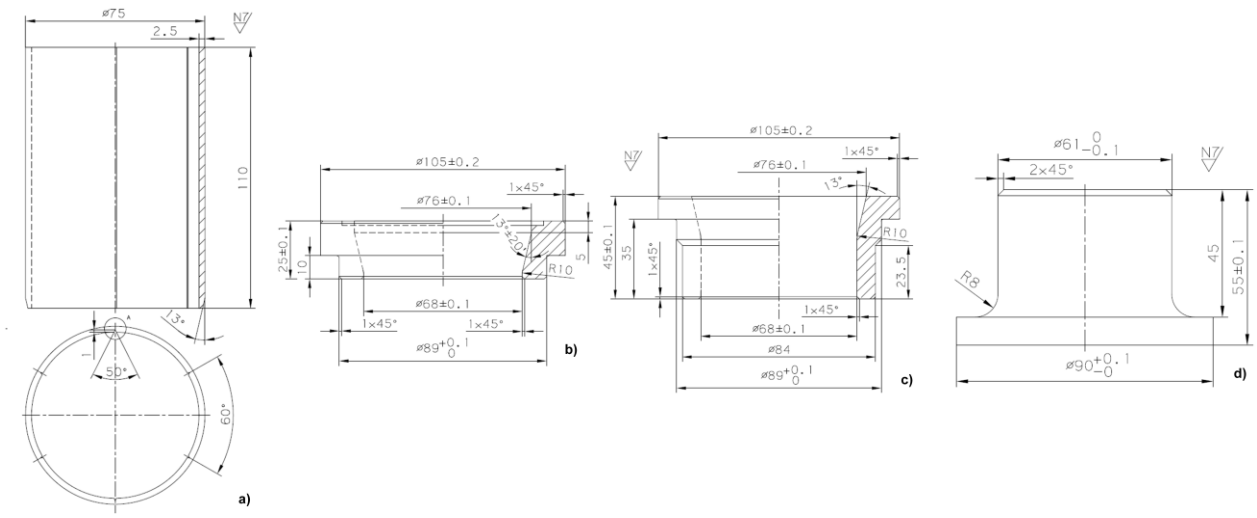

Figure 4 Dimensions of samples: a) Seamless grooved tube, b) Splitting tool, c) Smaller cone angle bushing and d) Larger cone angle bushing

Support tool (Fig. 5), manufactured from structural steel S355J2G3, was used as support of cone angle bushing and splitting tool during tests. This assembly is designed with oversized dimensions and kept initial dimensions after

series tests without any deformations. Easy disassembly of the supporting tool gives us the opportunity for fast change of samples between tests.

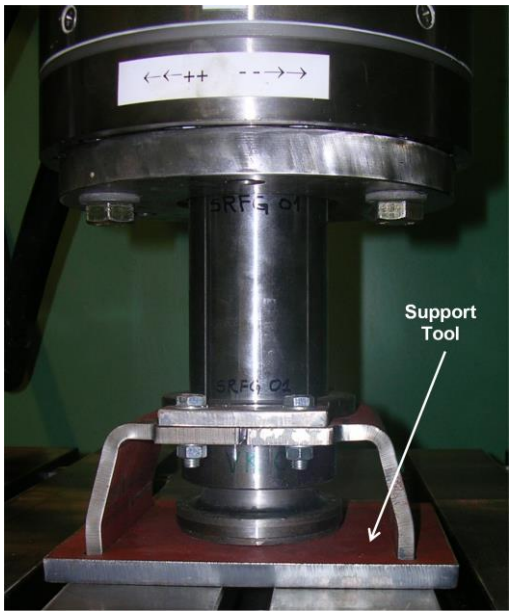

Figure 5. Position of assembly before the test

2.3. Quasi-static tests of combined absorber

Quasi-static tests were performed using the splitting tool shown in Fig. 6. The geometry of the splitting tool was chosen by using results of quasi-static investigations described Ref. [14]. The tool consists of a smooth cylindrical body and a flat base, with a large fillet radius that splits the tube along the grooves and causes the split ends of the tube to curl away.

Figure 6 Splitting tool

Force vs. stroke characteristics, F(h), obtained by experimental investigations of combined deformation process (extrusion and splitting) for tubes with grooves of length of 10 mm and 110 mm of energy absorption are shown in Fig. 7. For clarity, only one curve per particular specimen is presented. As expected, for a groove length of 10 mm the peak transmitted force is higher at the start of splitting process and significantly higher during the splitting of the tube wall until the end of deformation process. For this reason, the subsequent experimental investigations used tube samples with grooves along the full 110 mm length of inner wll, and the numerical modelling focussed on this.

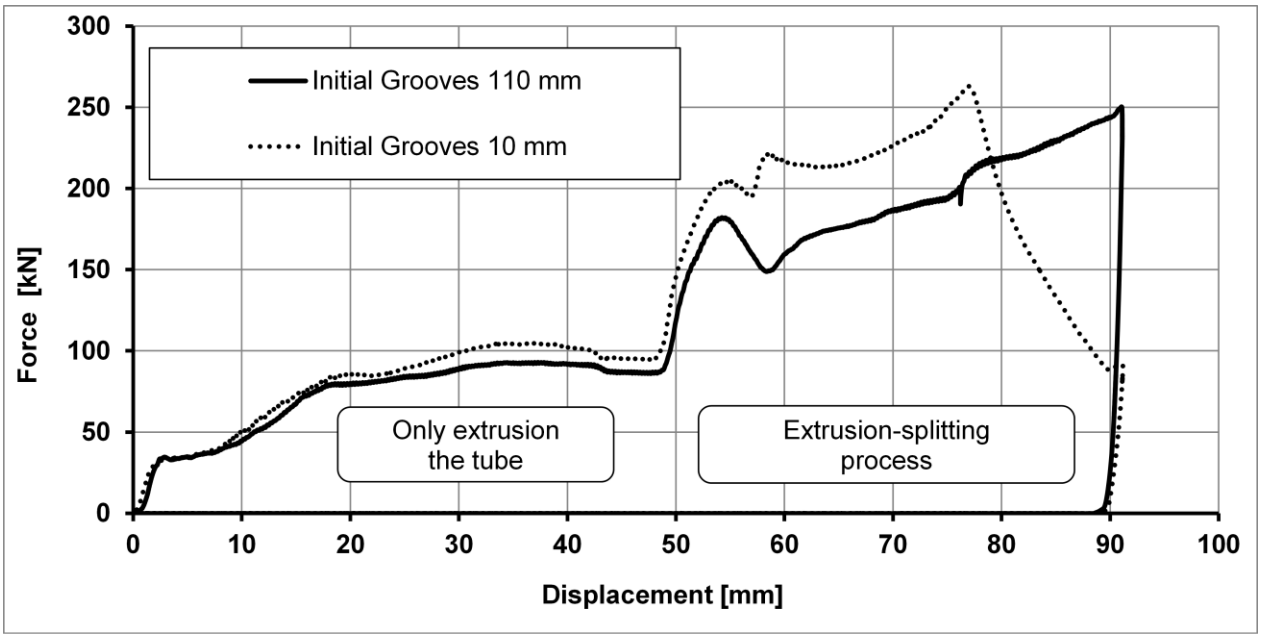

Figure 7 Diagram F(h) – different length of grooves

The force vs. stroke characteristics, F(h), were determined for the extrusion-only process (Fig. 8a), and for the combined extrusion-splitting process (Fig. 8b) at a piston speed of 1 mm/s.

a) Only extrusion process b) Extrusion-splitting process

Figure 8 Quasi-static tests

The maximum stroke of the test machine is 120 mm and the length of the sample is 110 mm. Tests were performed for a limited stroke of 90 mm with the aim to prevent blocking of the absorber or damage to the machine in extreme cases. The geometry of the tube (outer diameter, thickness and length) is designed to prevent buckling during the combined process.

3. Numerical simulations

Numerical simulations of the combined process of energy absorption were performed using finite element analysis. Validation of the numerical model would justify further development of this type of absorber using numerical simulations, accelerating the development phase and reducing the cost of full-scale tests prior to certification. Key parameters used for evaluation are: the shape of the force curve, values of force, and the shape of deformation. Because the ultimate shape of tube deformation is the consequence of large plastic deformations as well as contacts between the tube, cone bushing and splitting tool, nonlinear analysis using FEM is required. Based on previous experience in validation of numerical models, LS-Dyna software package was adopted. This software package has wide application in resolving dynamic nonlinear problems by using explicit integration. The nature of the experimental investigations corresponds to a quasi-static process, and the justification for using LS-Dyna is the achievement of the condition that the overall kinetic energy is less than 5 % of the internal energy [15].

3.1. Finite element model

Finite element method means discretization of the tube model, the cone bushing and the splitting tool whose geometric dimensions are fully in accordance with experimental model, Fig. 9a. Support tools are not modelled as it is considered that their influence is negligible.

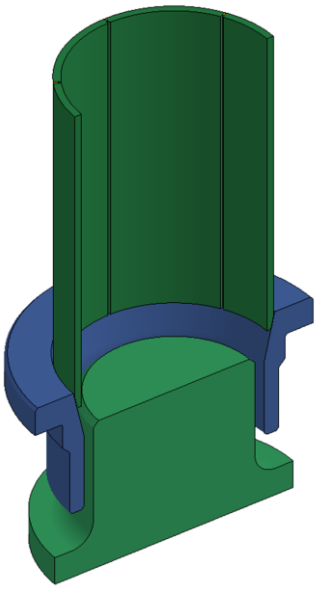

a) 3D model of combined absorber

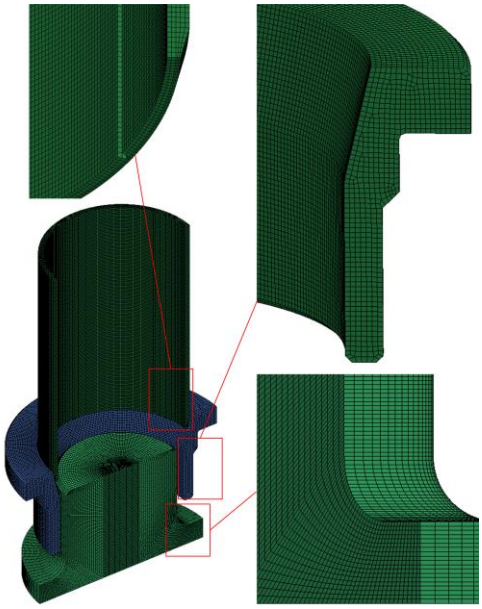

b) Meshed numerical model

Figure 9 Model of combined absorber

There is one plane of symmetry, which gives an option for discretization of one half of the model with the introduction of boundary conditions. Parts discretization was realized using 3D eight nodes solid elements. Mesh density is chosen so that it is larger in the initial grooves on the inner wall of the tube and in the contact zone, i.e., approximate dimensions of elements are 0.25x0.5x0.5mm and 0.5x0.5x0.75mm respectively, Fig 9b. Higher mesh density increases the time needed for numerical calculations but, at the same time, gives more accurately the stress and deformation field. Total number of 3D elements and nodes is 444540 and 504619 respectively.

3.2. Contact algorithm and boundary conditions

Modelling of contact should enable the interaction of parts that are not meshed, or to prevent the penetration of the nodes of one part into the elements of the other. Using LS-Dyna software package, it is possible to define different contacts, depending on the problem. For the interaction between the outside surfaces of the tube with the cone bushing as well as the interaction between the internal surfaces of the tube with the splitting tool, the contact "AUTOMATIC_ONE_WAY_SURFACE_TO_SURFACE" was used [16]. This type of contact prevents penetration of the nodes of tube into elements of cone bushing and splitting tool, especially at the zone of radius where abrupt change of the direction of the normal vector is expressed. The tube elements during deformation process touch each other, so for the tube another contact "AUTOMATIC_SINGLE_SURFACE" was applied. Adopted coefficients of friction are as follows: a) contact between the tube and the cone bushing, μ=0.15; and b) contact between the tube and the splitting tool, μ=0.25 [17].

In addition to the above boundary conditions of symmetry, the rest of boundary conditions are directed to the support tool, where the cone bushing and the splitting tool are constrained as stationary parts in zone where connected with other part of tools. Moving of nodes which are in the contact with machine piston is defined via option "PRESCRIBED_MOTION_SET", so that a movement is in the direction of their axis at speed of 1 mm/s. Except the defined movement and boundary of symmetry, the tube nodes are free and can move in the space under influence of cone bushing and splitting tool.

3.3. Material property

Mechanical characteristics of material P235T1, which was used for the tube, are defined by standard EN10028 [18] ANSYS Workbench non-linear material library. Numerical simulations were performed using bilinear characteristics of material [5]. Key material parameters of the tube material are shown in Table 1.

Table 1. Key characteristics of tube material

Component	Density [kg/m3]	Elastic modulus [MPa]	Tangent modulus [MPa]	Poisson ratio	Yield stress [MPa]	Failure strain	β
Seamless tube	7850	2.1e5	1.45e3	0.3	235	0.28	0.3

Bearing in mind the presence of large deformations, because of which it is necessary to take into account the reinforcing of material, this model of material "MAT_003_PLASTIC_KINEMATIC" was chosen, which is an isotropic, kinematic hardening model that can include strain-rate effects [19]. In the present work, however, the influence of strain rate is neglected, and the yield stress can be written in the following form

$$\sigma_y = \sigma_0 + \beta E_p \varepsilon_{eff}^p$$

where: σ_0 – yield stress, β – hardening parameter, ε_{eff}^p – effective plastic deformation, and E_p – plastic modulus of hardening is given in the following form

$$E_p = \frac{E_t E}{E - E_t}$$

where: E – Elastic modulus, E_t - tangent modulus.

During the deformation process, the tube tears along the grooves and the fracture criteria are defined using option "MAT_ADD_EROSION.

Mechanical characteristics of material 42CrMo4, which was used for the cone angle bushing and the splitting tool, are defined by standard EN10083 [20]. These parts were, however, modelled as rigid bodies.

4. Results

4.1. Extrusion of the tube

Fig. 10 shows the force vs. stroke diagram obtained by experimental investigations of the extrusion-only process, which presents the basis for evaluation of absorption power of combined absorber. The diagram contains three characteristic curves. The force increases gradually until a stroke of ≈ 30 mm, when the force reaches maximal value of ≈ 95 kN and remains at this value, with minor deviations, to the end of deformation process at a stroke of ≈ 90 mm. The force reaches its maximum value at the moment when the tube is passed through the cone bushing, so that the new diameter of the tube is equal to the smaller diameter of the cone bushing. At this moment, the end of the

tube, which has passed through cone bushing, is plastically deformed so there is no increase of force, i.e., the force remains at approximately 90 kN until the tube is fully used.

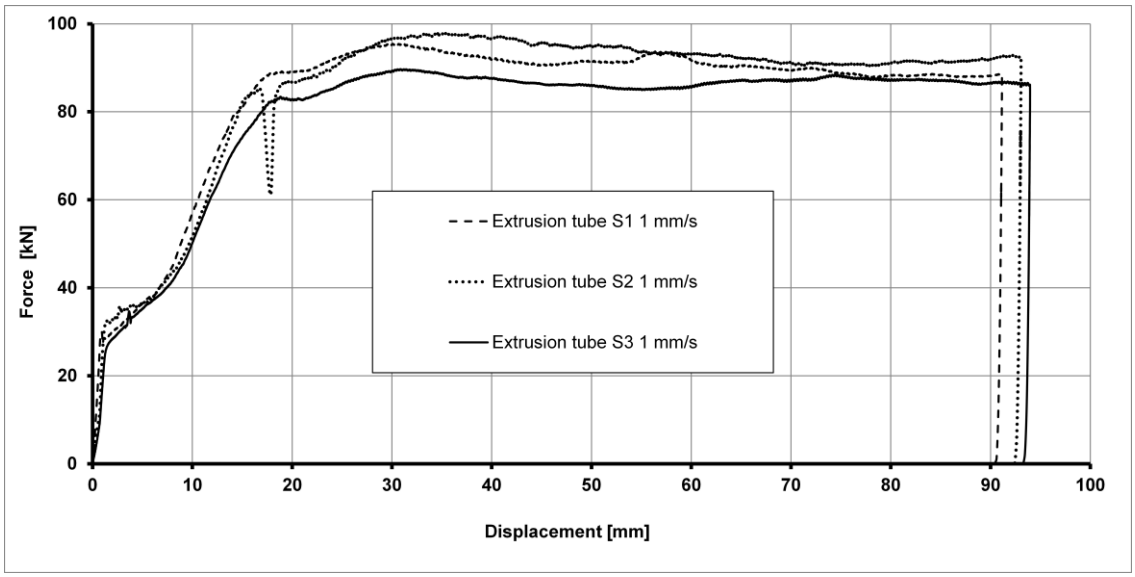

Figure 10 Force vs stroke – only extrusion of the tube

4.2. Extrusion-splitting of the tube

In the second phase of investigations three samples were tested using combined extrusion-splitting process. The force-versus-stroke diagrams obtained in this phase are shown in Fig. 11.

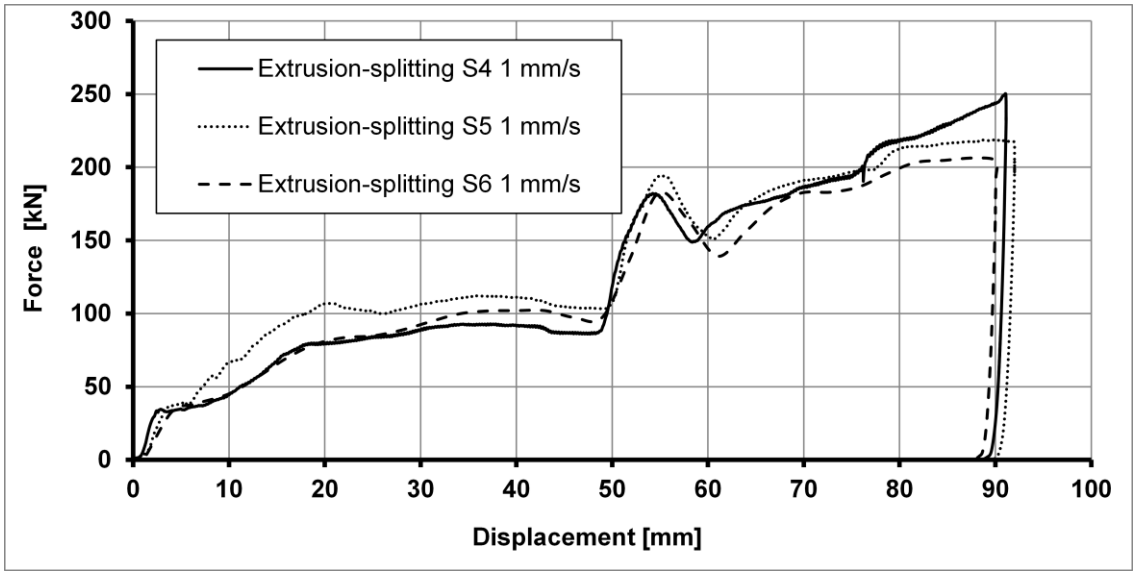

Figure 11 Force vs stroke – combined extrusion-splitting of the tube

In this diagram two separate phases of deformation can be clearly seen. First phase, for a stroke of ≈ 50 mm, refers to the extrusion process. This phase characterizes gradual increase of the force, to the moment when it reaches its maximum value of ≈ 90 kN at a stroke of ≈ 30 mm, after which the force remains at this value until a stroke of ≈ 50 mm. After this the splitting process starts at the end of the tube that has passed through cone bushing. Until the end of the deformation process (at a stroke of ≈ 90 mm), energy absorption is carried out in simultaneous extrusion-splitting process of deformation.

At the moment when the splitting process starts, at a stroke of 50 mm (the transition from the first phase to the second phase of deformation) the force increases from ≈ 95 kN to ≈ 180 kN. Then the tube begins to crack along the inner grooves, and the force decreases to ≈ 145 kN, at a stroke of ≈ 60 mm. From this point, the tube wall has controlled splitting into the strips along the longitudinal grooves and force increases gradually to the value of 220 kN at a stroke of 90 mm.

4.3. Numerical simulations

Fig. 12 shows the force vs. stroke diagram obtained by numerical simulation using LS-Dyna. In the diagram, two separate phases of deformation can be clearly seen. The first phase, until a stroke of ≈ 50 mm, represents the extrusion process. The second phase, from 50 mm to 90 mm, represents the parallel extrusion-splitting process. In the first phase, the force increases gradually until it reaches ≈ 100 kN, at a stroke of ≈ 30 mm. After that the force remains at this value, with minor deviations, until the end of the first phase, i.e., at 50 mm. At this moment, the end of the tube, which has passed through the cone angle bushing, touches the splitting tool and the force increases from 100 kN to 175 kN. This moment characterizes the first cracks when the process of controlled splitting of the tube into strips along the inner grooves starts and the force decreases to ≈ 150 kN (at a stroke of ≈ 58 mm). Up to a stroke of 90 mm, the tube continues to deform in parallel extrusion-splitting mode, and the force increases gradually to ≈ 200 kN.

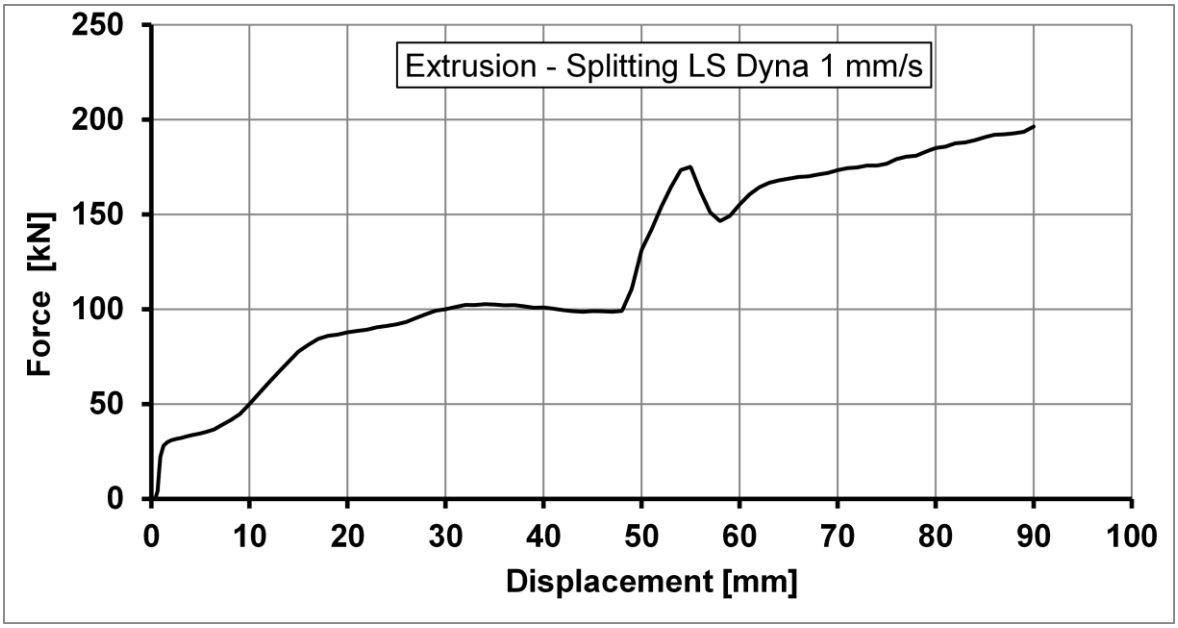

Figure 12 Force vs. stroke diagram – Numerical simulations

Fig. 13 shows the stress distribution and shape of deformation of the tube at a stroke of 90 mm. It is clear that the deformation of the tube obtained by numerical simulations is in accordance with the shape of deformation obtained by experimental investigations (see Fig. 7b).

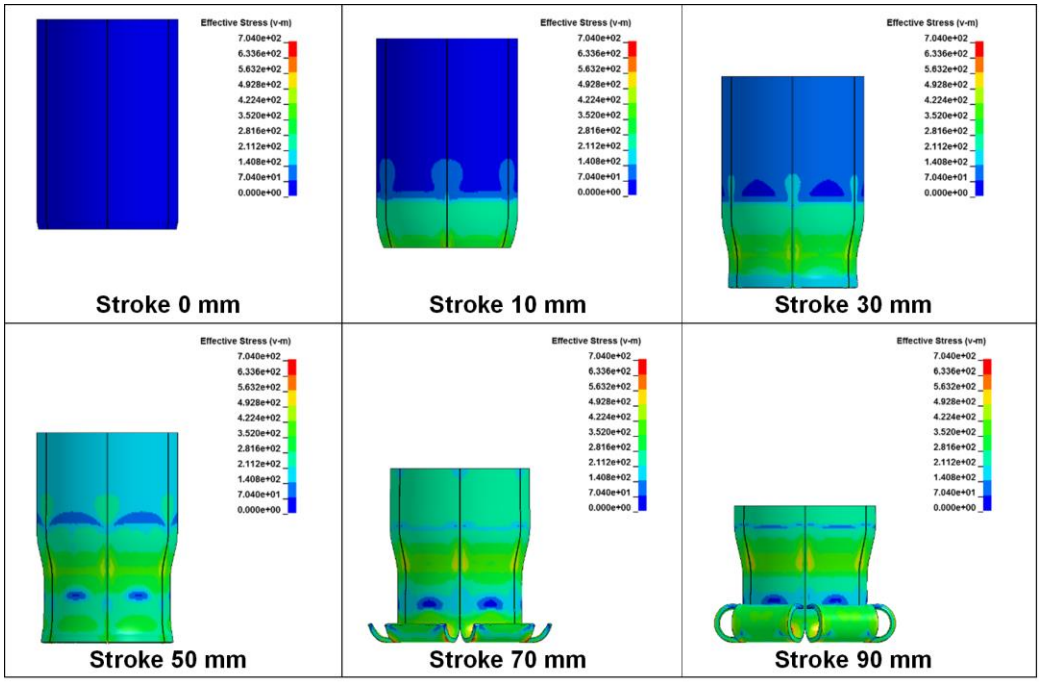

Figure 13 Stress distribution – Numerical simulations

4.4. Absorption power

Fig. 14 shows characteristic curves of the extrusion-only process (with samples marked as Item 1 in Fig. 3) and the extrusion-splitting process (with samples marked as Item 4 in Fig. 3). The curves are averaged respectively over the three tests for the extrusion-only process (see Fig. 9) and the three tests for the extrusion-splitting process (see Fig. 10). This clearly shows the difference between these two processes.

During the first phase, extrusion the tube, until ≈ 50 mm, there are no significant deviations of values of the force. Minor deviations are due to friction between elements, possible off-axis of the tube in relation to the cone bushing, as well as production quality (surface roughness) of the cone bushing, tubes and special splitting tool. In the second phase, between 50 to 90 mm, the area under the curve of the combined extrusion-splitting process is larger than the area under the curve of the extrusion-only process. This difference represents the increase of absorption power by using combined deformation process.

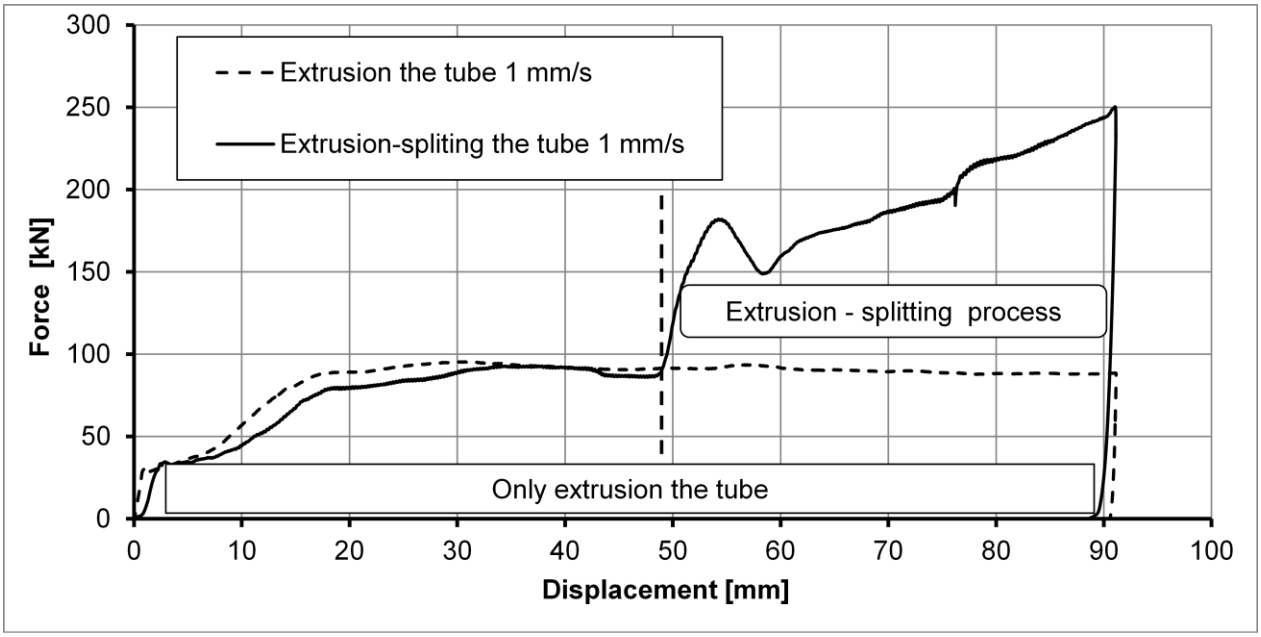

Figure 14 Absorption power

Table 2. Key parameters

Table 2 contains key parameters for evaluation of absorption power. Absorbed energy were calculated as a work of force at defined stroke (amount of absorbed energy is equal to area under curve):

$$\delta W = F_{av} \times \delta h$$

where F_{av} is the average value of the force at stroke h, δh is the increment of stroke, and δW is the work done (energy absorbed) over that increment.

The values in Table 2 indicate minor deviations in amount of absorbed energy in the first phase of deformation, i.e., deviations are ≈ 5 % (possible causes mentioned above). In the second phase of energy absorption, the amount of absorbed energy is more than twice as high for the combined process. Also, at the stroke of 90 mm, the combined process gives 55% higher absorption power than the extrusion-only process. The calculated value of total absorbed energy averages 10.96 kJ for the combined process and is estimated as 7.07 kJ for the extrusion-only process.

4.5. Validation of the numerical model

Fig. 15 shows curves of the combined process of energy absorption obtained by experimental investigations and numerical simulations. The force vs. stroke diagram shows good agreement. Deviations between the experimental and numerical results are at most ≈ 9.1 %. The larger deviations are in the second phase of deformation, between 60 and 90 mm, as would be expected given the complexity of the extrusion-splitting process. Friction between sliding surfaces, and crack growth (even with grooves present) introduce a stochastic element which causes an irregularity in practice, which leads to jerks in measured force that are not predicted by the finite element analysis.

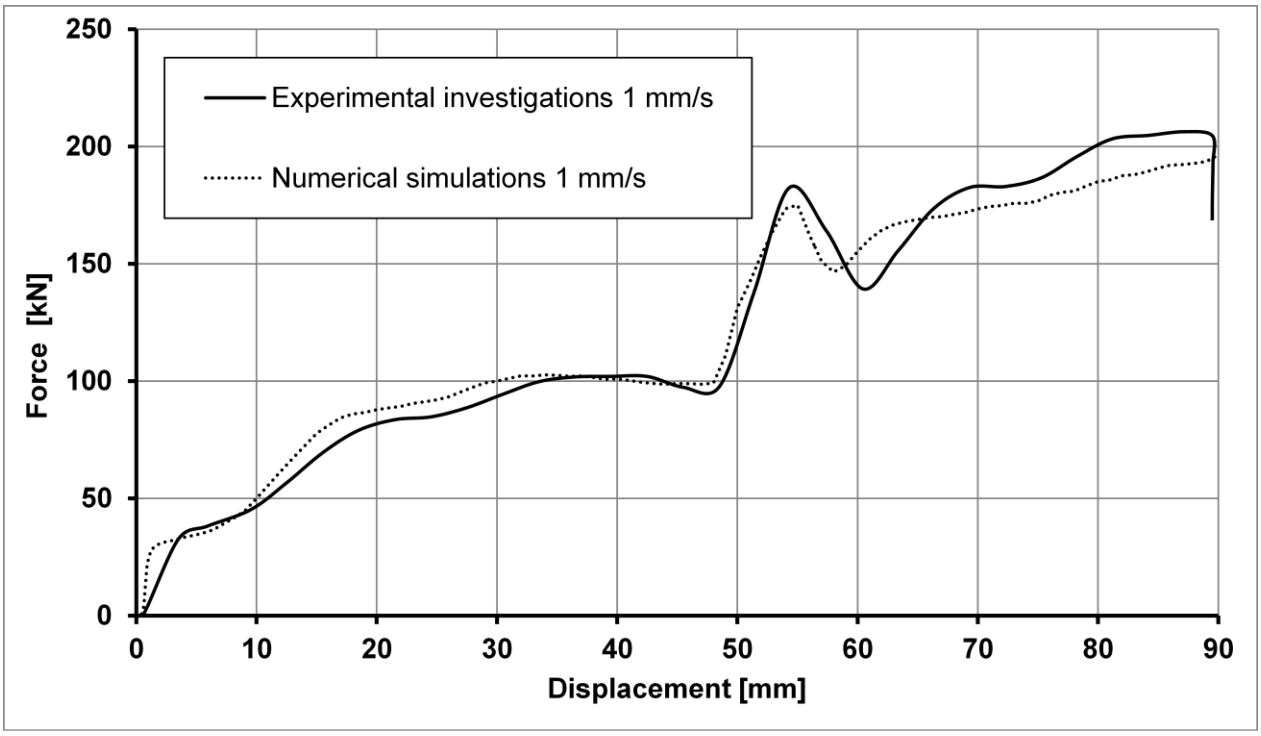

Figure 15 Validation of numerical model – F(h) characteristics

The shape of deformation predicted by the computer simulation matches that seen in the experiments, Fig. 16, so overall agreement between experimental and numerical results is very good, and the numerical model can be used as a basis for further development work of this type of absorption element. Minor deviation of presented dimensions measured on specimen and computational model are within acceptable tolerances. Designs costs, therefore, can be reduced to a large degree, as well as experimental investigations, which can be reduced to a final prototype test of full scale model of absorber.

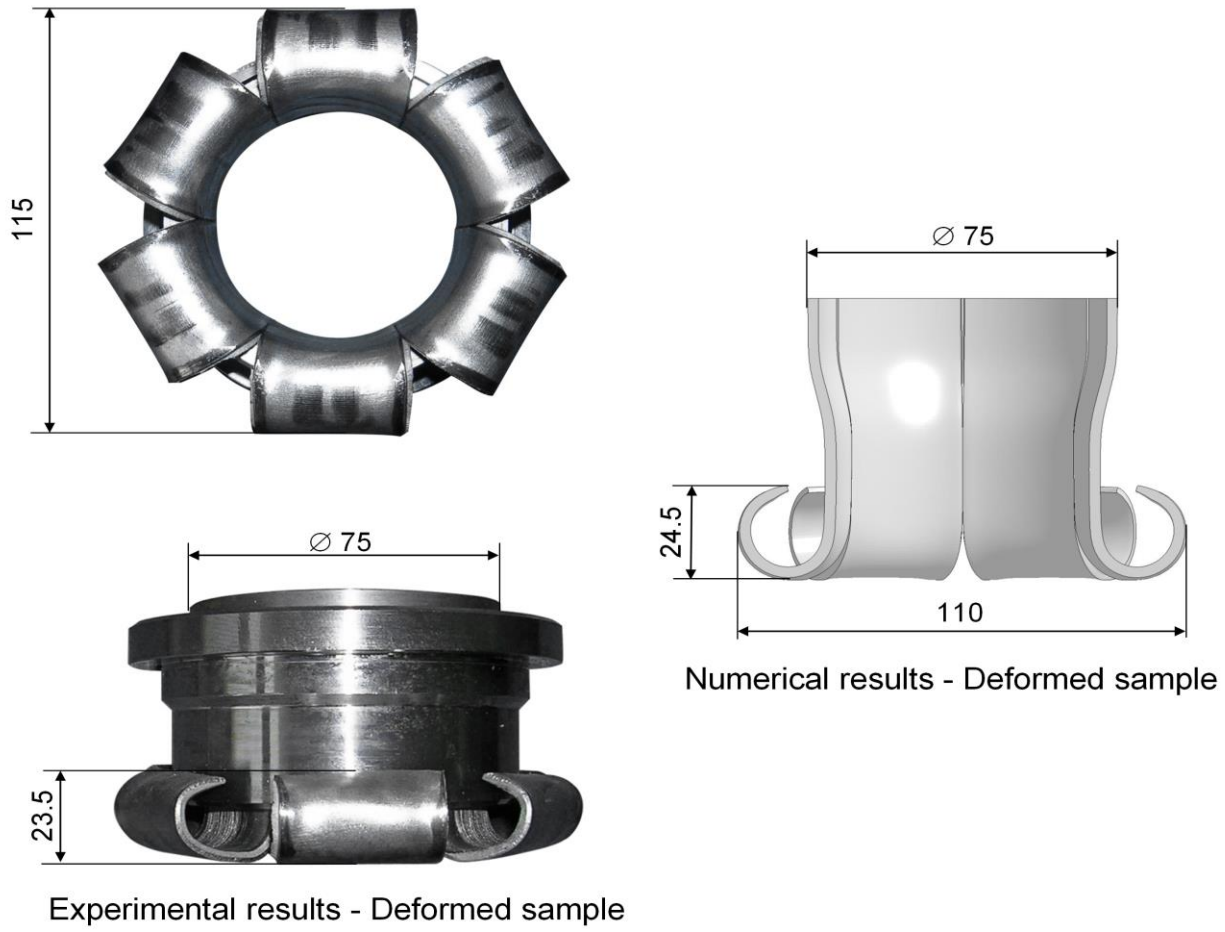

Figure 16 Validation of numerical model – shape of deformation

5. Conclusions

Trend of increasing of the speed in railway traffic requires application of applicable standards concerning improving active and passive safety. Many rail vehicles are not equipped with passive safety elements, so it is necessary to develop absorbers with compact dimensions that can satisfy the required absorption power and be installed during refurbishment without major work to the vehicle structure.

Results have been presented here of experimental and numerical study of a collision kinetic energy absorber that works on the principle of extrusion-splitting of a seamless tube. These show that the absorption power of the combined absorber is 55 % higher than the extrusion-only tube absorber. Experimental and numerical results are in a good agreement, which verifies the numerical model as a basis for further development of this type of absorption element. Development based on the numerical simulations in a large amount reduces costs and shortens the path from idea to prototype.

Higher absorption power, as well as compact dimensions, makes the combined absorber suitable for mounting on a new passenger and freight wagons, electro and diesel motor trains, locomotives and existing rail vehicles during refurbishment. It is possible to install absorber in a line with standard buffer or as a separate part on a rail vehicles equipped with an automatic train coupler.

References

1. EN 15227, Railway applications - Crashworthiness requirements for railway vehicle body, January 2008.
2. EN 12663-1, Railway applications - Structural requirements of railway vehicle bodies - Part 1: Locomotives and passenger rolling stock (and alternative method for freight wagons), 2015.
3. Simić G., Lučanin V., Tanasković J., Radović N., Experimental research of characteristics of shock absorbers of impact energy of passenger coaches, Journal of Experimental Techniques, Volume 33, Issue 4, page 29-35, 2009.
4. Lučanin, V., Tanasković, J., Milković, D., Golubović, S., Experimental Research of the Tube Absorbers of Kinetic Energy During Collision, FME Transactions, Volume 35, No 4, page 201-204, 2007.
5. Tanasković, J., Milković, D., Lučanin, V., Simić G., Experimental and numerical determination of tube collision energy apsorbers characteristics, FME Transactions, Volume 40, No 1, page 11 - 16, Belgrade, 2012.
6. Tanaskovic J., Lučanin V., Milković D., Simić G., Miloš M., Experimental Research of Characteristics of Modified Tube Absorbers of Kinetic Collision Energy of Passenger Coaches, Journal of Experimental Techniques, Volume 38, Issue 3, page 37-44, 2014.
7. Huang X., Lu G., Yu T. X., On the axial splitting and curling of circular metal tubes, International Journal of Mechanical Sciences, Volume 44, Issue 11, Pages 2369-2391, November 2002.
8. Niknejad A., Rezaei B., Hossein Liaghat G., Empty circular metal tubes in the splitting process – theoretical and experimental studies, Thin-Walled Structures, Volume 72, Pages 48-60, November 2013.
9. Atkins A. G., On the number of crack in the axial splitting of ductile metal tubes, International Journal of Mechanical Sciences, Volume 29, Issue 2, Pages 115-121, 1987.
10. Olabi A.G., Morris E., Hashmi M.S.J., Metallic tube type energy absorbers: A synopsis, Thin-Walled Structures, Volume 45, Issues 7–8, Pages 706-726, July–August 2007.
11. Chen D.H., Ushijima K., Estimation of the initial peak load for circular tubes subjected to axial impact, Thin-Walled Structures, Volume 49, Issue 7, Pages 889–898, 2011.
12. Kılıçaslan C., Numerical crushing analysis of aluminum foam-filled corrugated single and double circular tubes subjected to axial impact loading, Thin-Walled Structures, Volume 96, Pages 82-94, 2015.

13. Tanaskovic J., Milkovic D., Lucanin V., Miloradovic N., Experimental and numerical analysis of the characteristics of combined collision energy absorbers, Journal FACTA UNIVERSITATIS - Series Mechanical Engineering, Vol.10, No 2, pp. 125 – 136, 2012.
14. Tanaskovic J., Milkovic D., Lucanin V., Vasic Franklin G., Experimental investigations of the extrusion–splitting tube collision energy absorber, Thin-Walled Structures, Volume 86, Pages 142-147, 2015.
15. Baroutaji A., Gilchrist M.D., Smyth D., Olabi A.G., Analysis and optimization of sandwich tubes energy absorbers under lateral loading, International Journal of Impact Engineering, Volume 82, Pages 74-78, 2015.
16. LS-DYNA keywords user's manual Version 971 vol. I Livermore, CA: Livermore Software Technology Corp., 2007.
17. Podgornik B., Hogmark S., Pezdirnik, Comparison between different test methods for evaluation of galling properties of surface engineering tool surfaces, WEAR, Volume 257, Issues 7-8, Pages 843-851, October 2004.
18. EN 10028, Flat products made of steels for pressure purpose, 2010.
19. LS-DYNA keywords user's manual Version 971 vol. II Livermore, CA: Livermore Software Technology Corp., 2012.
20. EN 10083, Steels for quenching and tempering, 2011.

List of Figures

List of Tables